Application of a Six Degrees-of-Freedom Drag Model for Small Satellite Mission Development

Alex Reynolds
Department of Mechanical and Aerospace Engineering, Missouri University of Science and Technology
400 West 13th Street, Rolla, MO 65409-0050
amrnt7@mst.edu

Serhat Hosder and Henry Pernicka
Department of Mechanical and Aerospace Engineering, Missouri University of Science and Technology

ABSTRACT

For spacecraft in low-perigee orbits, atmospheric drag presents one of the largest uncertainties in dynamics modeling. These uncertainties are particularly relevant to small satellites, which often fly in the LEO regime and produce control forces and torques comparable in magnitude to drag. In this study, a six degrees-of-freedom orbital dynamics model with drag perturbations is developed, and several applications of the model are investigated. The model is used to evaluate differential drag dynamics for the MR and MRS SAT microsatellite pair, and the implications to collision avoidance and end-of-life procedures are discussed. Preliminary propellant usage estimates for the mission are also generated. A modified method for determining ballistic coefficient using relative satellite navigation data is introduced and compared to previous methods.

INTRODUCTION

Accurately determining and predicting the motion of space objects acting under the influence of atmospheric drag is critically important to mission planners, operators, and the space community as a whole. As the dominant perturbation acting on satellites at altitudes of less than 500 km, quantifying atmospheric drag's effects is essential to accurately modeling spacecraft proximity operations and formation flying. Additionally, as the need for enhanced space situational awareness (SSA) has become apparent, applications such as collision avoidance and orbit decay—both of which depend heavily on drag—have taken on increased importance. Acceleration due to drag on a spacecraft is typically written as

$$\mathbf{a} = -\frac{\rho A c_D ||\mathbf{v_{rel}}||^2}{2m} \frac{\mathbf{v_{rel}}}{||\mathbf{v_{rel}}||} \tag{1}$$

where $\mathbf{a}$ is the drag acceleration vector, ρ is the atmospheric density, A is the projected area of the spacecraft normal to the free stream, c_D is the drag coefficient, and $\mathbf{v_{rel}}$ is the relative velocity of the spacecraft with respect to the atmosphere. In scenarios where determining a spacecraft's area and mass individually may be difficult, the ballistic coefficient, β, is sometimes used instead and defined such that

$$\beta = \frac{A c_D}{m} \tag{2}$$

and is representative of the perturbing effect drag will have on an individual spacecraft.

Despite its seemingly innocuous form, atmospheric drag is one of the most difficult spacecraft perturbations to quantify. Even when using state-of-the-art models for atmospheric density and the drag coefficient, large errors can arise, which only tend to grow as spacecraft orbits are propagated. In general, drag modelling is broken into two components: particle-surface interaction and atmospheric density modelling. While a detailed examination of these two topics lies beyond the scope of this paper, a brief overview is presented in order to provide background to the reader.

Particle-surface interaction mostly concerns accurately estimating the drag coefficient. However, the drag coefficient is not constant for a spacecraft in the upper atmosphere – it will change according to the spacecraft's attitude and altitude. For spacecraft flying in LEO, it is common to assume that flow is rarefied and particle-surface interactions dominate over particle-particle interactions. These interactions can vary based on the atmospheric composition at a given altitude, surface properties of the spacecraft, and the angle of incidence with which they strike a given surface, all of which conspires to make correctly estimating drag coefficient a difficult task. In practice, the drag coefficient is roughly bounded between two and four, and is typically assumed to be 2.2 in cases where it is unknown or a high-accuracy estimate is not required.[1]

Even more so than the drag coefficient, atmospheric density is dominated by uncertainties that serve to make good estimation difficult. In fact, atmospheric density is

the single largest contribution to error in orbit determination applications.[2] Uncertain parameters in atmospheric density estimation include solar flux, atmospheric composition, latitude, longitude, and seasonal effects, all of which contribute to a widely acknowledged 10-15% uncertainty in density models.[2] As a result, the accurate estimation of atmospheric density has been an active area of research for many years, and a variety of models are in use – each with its own advantages and disadvantages. These models typically combine an analytical approach with empirical satellite data in order to best estimate atmospheric conditions at some epoch. Among these models, the DTM-2013, JB2008, and NRLMSISE-00 models are some of the most widely used.[3]

Taken together, drag and its associated variations affect many aspects of a spacecraft mission in LEO. The duration of satellite operations can often vary greatly depending on the conditions of the atmosphere at the time of deployment.[3] Additionally, evidence has shown that satellites, particularly small satellites, become more difficult to track when drag is not properly accounted for.[4] Drag has also found application as a formation control method for large satellite constellations–one well-known example being the Planet Labs constellation.[5]

The focus of the effort described in this paper is on the application of drag modeling to relevant issues facing the small satellite community, particularly in the university setting. As such, the paper is divided into two parts. In the first, the development of a medium-fidelity drag model with applications to mission and algorithm design is discussed. The missions currently in development at Missouri S&T are also introduced, and potential applications of the model to each are outlined. In the second, methodologies and results related to the model's implementation on the MR and MRS SAT microsatellite mission are presented. Numerical analysis is performed and compared to higher-fidelity STK results.

MODEL DEVELOPMENT

Despite its importance to successful mission planning and development, drag is sometimes neglected in the university setting. At Missouri S&T, high-fidelity software packages, such as STK, which incorporate a variety of perturbation models, are used during the initial proof-of-concept and final mission verification phases. However, a large portion algorithm design and mission planning functions are performed on platforms like MATLAB. While features, such as MATLAB *MexConnect*, enable users to link software to higer-fidelity modeling applications, such as STK, the connection is often inefficient and impractical for algorithm development, particularly in cases where Monte Carlo simulations are required. Additionally, the learning curve associated with such analysis tools can preclude less experienced students from contributing fully to design work.

As a result of these constraints, team members are often left to develop their own drag models to suit their needs, which may vary widely in accuracy and applicability. Most often, these models rely on an exponential estimate of atmospheric density, and may not account for important factors, such as Earth's rotation and oblateness. In many cases, these models are used to tune control constants, run Monte Carlo simulations, and evaluate relative dynamics, which can, in application, lead to inconsistencies between algorithms. For low-altitude small satellites, such as those developed by the Missouri S&T Satellite Research Team (M-SAT) and other universities, these inconsistencies (coupled with the overhead of developing and verifying a simple drag model) can have a negative impact on mission design and development.

The orbital dynamics and drag model that is a focus of this work was developed to address these concerns. As a tool designed to meet a variety of applications, it is based on a modular, flexible design that allows for as many potential use cases as possible–including adoption by other universities and organizations outside of Missouri S&T. While currently only available in MATLAB, future work could realize a similar model developed in C++.

At its highest level, the model propagates six degrees-of-freedom motion based only on two-body dynamics and atmospheric drag. Density is determined using the implementation of the 1976 Standard Atmosphere developed by Brent Lewis, and available on MATLAB File Exchange.[6,7] This model, while less accurate than other, more modern atmospheric models, was chosen because of the speed and simplicity it offers. In the mission planning and design phase, the solar flux and seasonal variation considerations offered by other models are typically not necessary.

Earth is assumed to be spherical for gravity calculations, but its radius (and therefore the reference altitude of the spacecraft) is allowed to vary with latitude. A simplified atmospheric rotational model, in which the atmosphere rotates with Earth, is also incorporated. MATLAB's *ode113* is used to update the spacecraft state over discrete time intervals, where the spacecraft state is a 13-element vector given by

$$\mathbf{x} = \begin{bmatrix} \mathbf{r} \\ \mathbf{v} \\ \mathbf{q} \\ \boldsymbol{\omega} \end{bmatrix} \tag{3}$$

and $\mathbf{r}$, $\mathbf{v}$, $\mathbf{q}$, and $\boldsymbol{\omega}$ represent the spacecraft position and velocity vectors, attitude quaternion, and angular velocity vector, respectively. At every time interval, the state

is updated according to

$$\dot{\boldsymbol{x}} = \begin{bmatrix} \mathbf{v} \\ \mathbf{a} \\ \dot{\boldsymbol{q}} \\ \boldsymbol{\alpha} \end{bmatrix} \tag{4}$$

where $\mathbf{v}$, $\mathbf{a}$, $\dot{\boldsymbol{q}}$, and $\boldsymbol{\alpha}$ represent the spacecraft velocity and acceleration vectors, rate of change in the quaternion with respect to time, and angular acceleration vector, respectively.

To maximize the number of use cases, the model is designed such that it can be invoked in a number of ways. Using the built-in features of MATLAB, the model is overloaded to be run as a script, where the operator specifies initial parameters directly, or as a function, where the operator passes initial conditions to the model to perform a single propagation. A companion function was also developed to return the forces and moments on a spacecraft, given its position and velocity. An easily modifiable "custom dynamics" script was also incorporated into the design, which further enhances functionality by enabling users to add thrusters, torque coils, and additional perturbations without having to modify the model itself.

As computational speed is one key element of the model, it is designed to achieve maximum efficiency without sacrificing performance. Firstly, the model tracks a variety of global parameters, such as the 1976 Standard Atmosphere table, and generates them only on its first run. This is particularly important for maintaining speed when called as a function multiple times, as applied to the ballistic coefficient estimation outlined in later sections. The model also uses linear interpolation and creative indexing to avoid doing a vector search of the 1976 Standard Atmosphere table—a lengthy procedure that would drastically decrease performance.

To make the development suite user-friendly, several visualization and debugging features are incorporated. One such feature is the attitude GIF generator, which automatically generates and displays a GIF of the attitude and position of the spacecraft in user-specified time steps. Figure 1 shows this feature in use.

APPLICATION

APEX and M^3

The M-SAT Advanced Propulsion Experiment (APEX) and Multi-Mode Mission (M^3) missions are two CubeSat missions currently in development at Missouri S&T. As companion missions, they both seek to demonstrate the use of a multi-mode thruster that is capable of switching between chemical and electrical thrust modes as needed. The M^3 Mission, sponsored by NASA's Undergraduate Student Instrument Project and the CubeSat Launch Initiative, seeks to demonstrate the thruster's ability to operate on-orbit. The APEX mission, which is currently competing in Phase A of the AFRL University Nanosatellite Program (UNP), has the potential to launch soon after, and will seek to quantify the thruster's performance on-orbit.

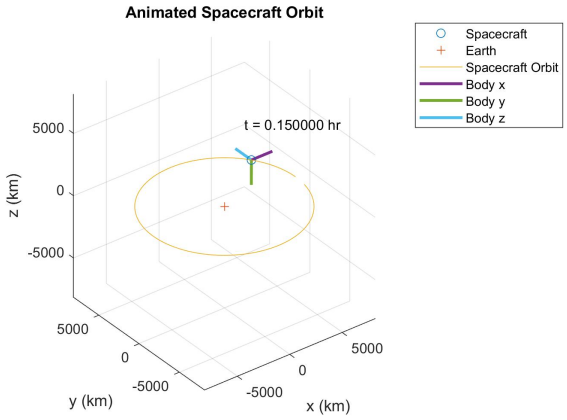

Figure 1: The Drag Model GIF Generator

For both missions, accurately quantifying and predicting perturbations on the spacecraft will be critical to mission success. The 3U M^3 mission is likely to deploy at an altitude of around 300 km, where the perturbing effects atmospheric drag will be strong and re-entry will occur quickly. Additionally, the satellite will only use a permanent magnet and set of four hysteresis rods to detumble, which means that atmospheric drag will likely play a large role in determining the satellite's detumbling time, and, therefore, operational lifetime. In such a case, small errors in drag calculation can have unforseen consequences that risk mission success, and the need for fidelity beyond a simple exponential model becomes apparent.

The APEX mission, on the other hand, is tasked with quantifying the performance of the multi-mode thruster in both chemical and electric mode —- a challenge, as the thrust produced in electric mode is on the order of several millinewtons. Similar to the M^3 mission, accurately quantifying drag perturbations on the spacecraft is essential to developing an operable mission, yet the framework for determining such perturbations must be fast and flexible enough to support Monte Carlo simulations on various orbits, along with the development thruster and attitude control algorithms.

MR and MRS SAT

The MR and MRS SAT pair of microsatellites form a technology demonstration mission developed by M-SAT, currently in Phase B of the UNP program. The mission is

intended to increase the TRL of stereo vision-based autonomous navigation systems, and consists of two satellites, "MR SAT," a 50 kg inspector satellite and "MRS SAT," a 10 kg target spacecraft. After deploying in mated formation from the ISS, the pair will separate on-orbit, and MR SAT will attempt to perform proximity operations about MRS SAT. These operations will consist of a trailing mode, in which MR SAT will attempt to maintain a position ten meters behind MRS SAT, and circumnavigation mode, in which MR SAT will circumnavigate MRS SAT for two full orbits at the same distance.

As a satellite pair performing proximity operations in LEO, the two microsatellites form an excellent test case for the aforementioned drag model. In the following sections, the model is used to evaluate differential drag on the pair and estimate the ballistic coefficient of MRS SAT, from which conclusions are drawn about propellant consumption and collision avoidance.

DIFFERENTIAL DRAG MODELING

Differential drag refers to the difference in drag force between two or more spacecraft, and is an important parameter to consider for spacecraft performing proximity operations in a LEO environment. While differences in drag can be caused by different spacecraft altitudes and ballistic coefficients, differential drag analyses are most typically concerned with modifying (in the case of formation control) or examining (in the case of proximity operations) the effect of differences in ballistic coefficient.

As spacecraft orbit, drag continuously acts on them in a direction roughly opposite the velocity vector. This drag serves to decrease the orbital energy of the spacecraft, and is proportional to the spacecraft's ballistic coefficient – a measure of how much drag will influence a given spacecraft. For two hypothetical satellites in LEO, this would cause a satellite with a larger ballistic coefficient to lose energy faster, decreasing its semimajor axis and altitude. Counterintuitively, this has the effect of increasing satellite speed, as orbital period decreases with decreasing semimajor axis. This effect of increasing velocity by increasing ballistic coefficient is the key to differential drag analysis and differential drag control methods.

MR and MRS SAT Mission

For the MR and MRS SAT mission, which consists of two satellites with different ballistic coefficients performing proximity operations in a near-ISS orbit, differential drag effects are critical. While MRS SAT has no translational control, MR SAT relies on twelve cold-gas thrusters to perform trailing and circumnavigation operations. Because any number of failures could occur, such as MR SAT prematurely consuming all of its propellant, it is impossible to fully guarantee that MR SAT will have translational control while in the vicinity of MRS SAT, raising the possibility of a collision. Should the two collide with enough velocity to create orbit debris, the implications for other spacecraft in similar orbits could be catastrophic. Similarly, a broken camera or chipped solar panel resulting from a collision could put the mission in jeopardy.

The analysis detailed in this section seeks to answer two questions:

1. What is the behavior of the two satellites after MR SAT loses translational control, under nominal conditions?
2. What is the probability that the two satellites will collide, under the same nominal conditions?

In order to do so, it makes use of the drag model developed in earlier sections.

Methodology

For this analysis, a simulation was constructed using the aforementioned drag model. MR and MRS SAT were assumed to be in circumnavigation mode – the most likely mode for the pair to be in if MR SAT's propellant or power become depleted. Because a large number of parameters in the simulation, such as the pair's initial relative position and drag coefficients, are uncertain, a Monte Carlo framework was used to vary the pair's initial relative position and velocity and ballistic coefficient.

To eliminate as many uncertainties as possible, MRS SAT was constrained to a circular orbit at an altitude of 400 km, and the same initial position was used for MRS SAT on every Monte Carlo run. From this initial position, MR SAT's relative position and velocity vectors were generated.

Generating the relative position and velocity of MR SAT was made difficult by the inherent properties of a circumnavigation orbit – in such an orbit, MR SAT performs exactly one revolution around MRS SAT for every orbit about Earth. This configuration minimizes propellant use, but also means that the initial relative position and velocity are coupled to one another. To best understand the behavior of the two satellites, a simplified approach was taken, wherein MR SAT's relative position and velocity were generated for a circular orbit about MRS SAT inclined 45 degrees in the LVLH frame. Position and velocity were coupled according to an angle, θ. In this approach, MR SAT's relative velocity vector was assumed perpendicular to the relative position vector, and given a direction consistent with a circumnavigation orbit. The relative position and velocity vector magnitudes were assumed constant, consistent with a ten meter circumnavigation orbit. The angle θ was generated according to

a uniform, Latin Hypercube distribution between $\theta = 0$ and $\theta = 360$ degrees. Figure 2 demonstrates the coupling of relative position and velocity.

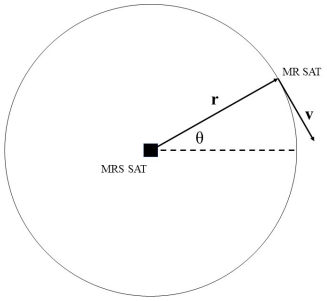

Figure 2: Coupled Relative Position and Velocity

The ballistic coefficients of MR and MRS SAT were also considered uncertain in the simulation. Using known values for the cross-sectional area and mass, and an assumed drag coefficient of 2.2, MR SAT's ballistic coefficient was estimated to be three times that of MRS SAT. These values were generated according to a normal distribution, with a standard deviation of 2%.

Monte Carlo simulations were run with 10, 50, 100, 500, 1000, and 5000 samples to demonstrate convergence of the model. For each run, the along-track separation of MR and MRS SAT were recorded at 1, 3, 5, and 10 hours. While angular, rather than linear, separation is typically used in differential drag analyses, linear, along-track separation was chosen because it provided a more intuitive sense of the separation between the spacecraft. Additionally, the short propagation time and, therefore, small separation distance meant that along-track separation would be a good estimate of the true separation between the spacecraft. For each set of Monte Carlo runs, the mean was collected, and the 95% confidence interval was estimated using the bootstrap method. Additionally, the relative positions of MR and MRS SAT were tracked in ten second intervals to record any possible collisions between the pair. If, at any point, the magnitude of the relative position vector between the pair dropped below one meter, a collision was recorded for that run.

Results and Analysis

Table 1 shows the separation between MR and MRS SAT for each Monte Carlo set. Note that a positive separation indicates that MR SAT is ahead of MRS SAT in the along-track direction, as is the case for every result in Table 1. Additionally, it is worth noting from Table 1 that the 95% confidence interval size found using the bootstrap method decreases as the number of samples increases – a sign that the model is converging as expected.

Figures 3-6 show the separation between MR and MRS SAT from the 5,000 sample Monte Carlo run, divided into bins to reflect how often each separation distance occurred. They also reveal an interesting result – given a normal distribution for ballistic coefficient of both satellites, and a uniform distribution of θ, the pair tend towards the maximum possible separation from one another in both along-track directions. While this bi-modal distribution is most noticeable in Figure 3 (separation after one hour), it is still present in Figure 6 (separation after 10 hours). The distribution is also reflected in the collision data – during the 5,000 sample Monte Carlo run, there were no cases where MR and MRS SAT collided.

Table 1: Spacecraft Pair Separation After Ten Hours

Samples	Mean Separation (m)	Conf. Interval (m)
10	3785	[3570, 4001]
50	3801	[3746, 3856]
100	3852	[3808, 3897]
500	3828	[3807, 3850]
1000	3811	[3787, 3835]
5000	3815	[3807, 3823]

Taken by themselves, Figures 3-6 reveal much about the pair's behavior – initially, separation between MR and MRS SAT is dominated by the initial conditions. Then, over time, differences resulting from ballistic coefficient cause separation to tend toward a normal distribution. The theory that initial conditions between the spacecraft dominate their separation is supported by Figure 7, which shows a scatter plot of separation after 10 hours plotted against θ. However, neither plot offers any indication as to why this extreme bi-modal distribution occurs.

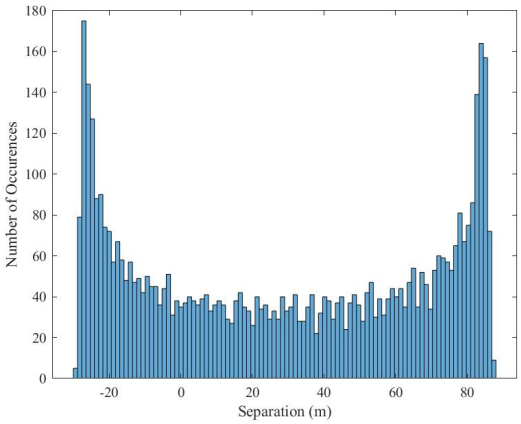

Figure 3: Satellite Pair Separation After One Hour

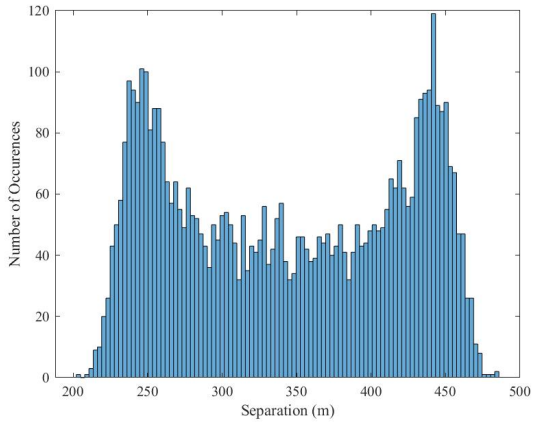

Figure 4: Satellite Pair Separation After Three Hours

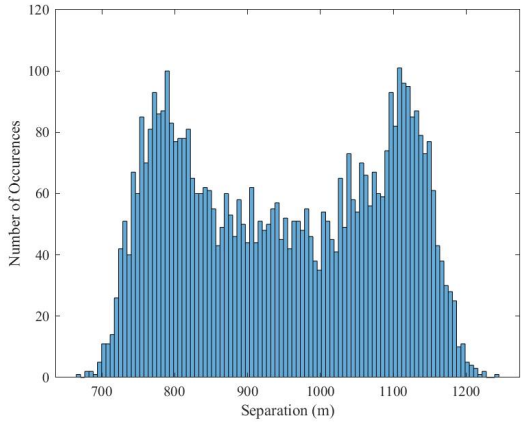

Figure 5: Satellite Pair Separation After Five Hours

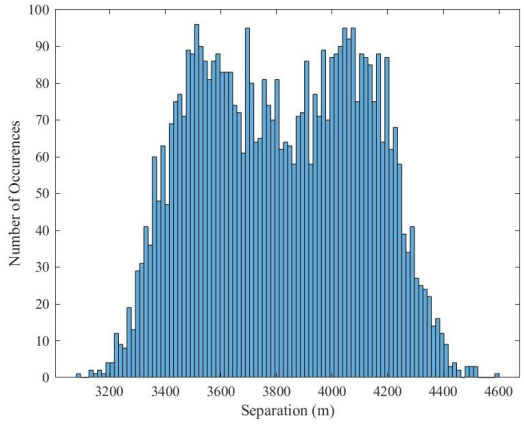

Figure 6: Satellite Pair Separation After Ten Hours

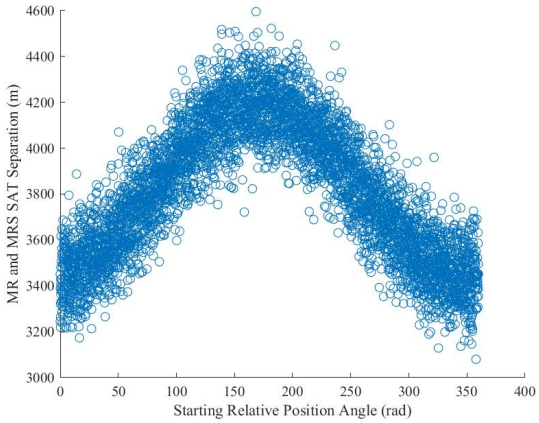

Figure 7: Satellite Pair Separation Based on θ

In order to further investigate this phenomenon, position and velocity were decoupled in several subsequent simulations. In the first, the ballistic coefficients of MR and MRS SAT were held fixed, along with MR SAT's relative position and velocity vector magnitudes. The directions of each vector were then generated independently within the plane of the circumnavigation orbit, according to a uniform distribution. Figure 8 shows the results of this simulation after 1 hour, from a Monte Carlo run of 1,000 samples.

In addition to the decoupled position and velocity simulation, two simulations were conducted on position and velocity independently. In these simulations, the ballistic coefficients of each satellite were constrained to the same value, and were not allowed to vary. In the first, MR SAT's relative position was varied according to θ, while its relative velocity was fixed at zero. In the second, MR SAT's relative position was fixed at zero, while relative velocity was varied according to the same θ. The results for MR and MRS SAT's separation after ten hours based on independent position and velocity simulations are shown in Figures 9 and 10, respectively.

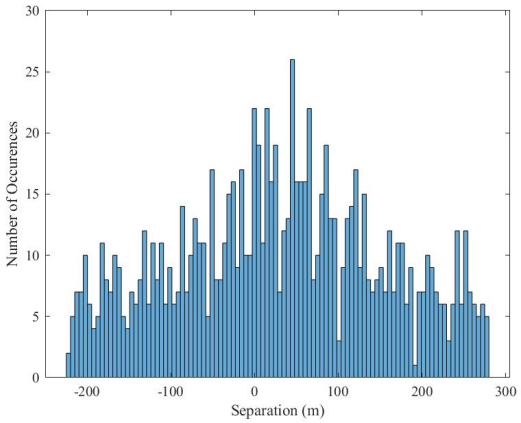

Figure 8: Satellite Pair Separation After One Hour

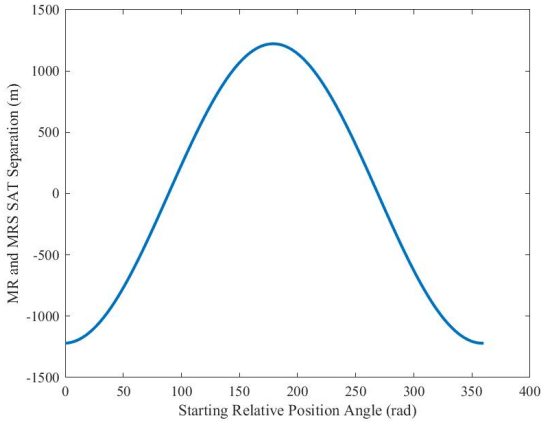

Figure 9: Separation Based on Relative Position After Ten Hours

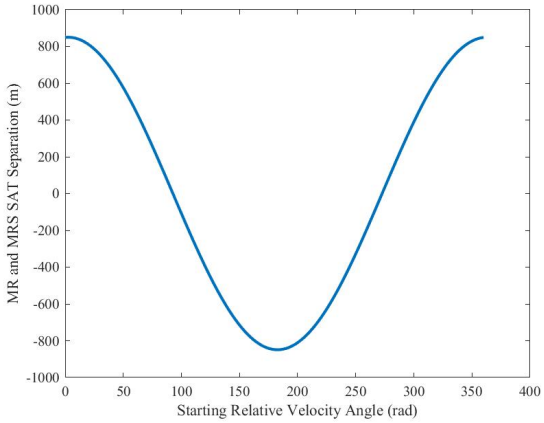

Figure 10: Separation Based on Relative Velocity After Ten Hours

As Figure 8 demonstrates, the tendency of the spacecraft to drift apart from one another is the result of coupled position and velocity. Figures 9 and 10 reinforce this conclusion. Although the effects of MR SAT's relative position (Figure 9) and relative velocity (Figure 10) act contrary to one another for the same θ, both tend to drive MR SAT away from MRS SAT. Therefore, when coupled, the net effect is to cause MR and MRS SAT to drift apart – even when the two have the same ballistic coefficient.

Differential Drag Conclusions

Based on the results outlined above, a number of interesting conclusions can be drawn:

1. The coupling of position and velocity necessary to achieve circumnavigation orbits tends to drive the inspector and target spacecraft apart once propulsive capability is lost.
2. Even several hours after propulsive capability is lost, separation between the two spacecraft is dominated by initial conditions.
3. Within three hours, differences in ballistic coefficient always cause MR SAT to drift ahead of MRS SAT. Therefore, any collisions that may occur between the pair are limited to the first several hours after control loss.

The first conclusion is also supported by the collision data. Even in the 5,000 sample Monte Carlo simulation, with an initial separation distance of ten meters, the two spacecraft never passed within one meter of one another. While this result does not preclude the need for end-of-life maneuvers and safety precautions between the MR and MRS SAT spacecraft pair, it does provide a high-level assurance that the two craft are unlikely to collide on orbit – even in the event of a sudden power or propulsion loss on MR SAT.

Propellant Estimates

In addition to its implications for collision avoidance, differential drag has an impact on the MR and MRS SAT propellant budget. Just as with collision avoidance, the properties inherent to a circumnavigation orbit tend to cause the pair to drift apart, with MR SAT's thrusters as the only means to maintain the formation and execute the mission.

In order to study the effects of differential drag on MR SAT's ability to successfully station-keep, a linearized analysis of the total ΔV required for the mission was conducted. In this analysis, it was assumed that the velocity necessary for MR SAT to maintain its desired relative position can be linearly approximated by

$$\boldsymbol{v} = \frac{d\boldsymbol{r}}{dt} \approx \frac{\Delta \boldsymbol{r}}{\Delta t} \tag{5}$$

where $\Delta \mathbf{r}$ and dt are small. This linearized velocity was then integrated over the length of the mission to

determine MR SAT's total propellant usage.

In order to successfully perform this linearized analysis, MRS SAT's position was propagated for two full orbits – the estimated duration of the mission. From this propagation, MR SAT's desired relative position and velocity were determined at every point on the orbit. As the linear assumption is only valid for small Δt values, MR SAT's orbit was propagated with a Δt of five seconds. At every time step, MR SAT was placed in its desired position, then propagated forward by Δt. At the end of the propagation, MR SAT's relative position was compared to its desired relative position at that time, such that

$$\Delta \boldsymbol{r} = \boldsymbol{r}_{desired} - \boldsymbol{r}_{actual} \tag{6}$$

This $\Delta \boldsymbol{r}$ was then used to calculate $\frac{\Delta \boldsymbol{r}}{\Delta t}$ for that time step. After $\frac{\Delta \boldsymbol{r}}{\Delta t}$ was recorded, MR SAT was set to its desired position and velocity at the start of the next time step, and the process was repeated for every time step until the three hour limit was reached. This analysis was conducted at a variety of potential starting positions, denoted by θ, for MR SAT in order to determine if any orientation presented a Δv advantage. The results are shown in Figure 11.

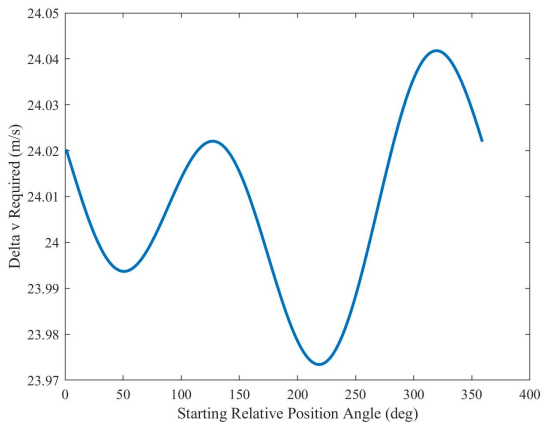

Figure 11: Propellant Required for MR SAT Circumnavigation of MRS SAT

As the figure shows, propellant usage is not constant for the entire range of potential relative starting positions for MR SAT, and certain orientations do present a possible advantage. However, MR SAT possesses a total ΔV of just 24.9 m/s, which potentially indicates that two circumnavigation orbits will leave a very small propellant margin for the mission.

BALLISTIC COEFFICIENT ESTIMATION

One aspect of the MR and MRS SAT mission success criteria (MSC) is the successful estimation of MRS SAT's ballistic coefficient using only relative position data generated from MR SAT's stereoscopic imager. In order to accomplish this, MR SAT must be able to successfully perform proximity operations about MRS SAT using its stereoscopic imager. Then, using the relative position data collected, M-SAT engineers must demonstrate successful processing of the data into a ballistic coefficient estimation, either onboard MR SAT or using downlinked data. The effort described in this section focuses on the latter approach.

Orbital debris from man-made objects is a growing problem recognized by a variety of organizations worldwide. As of 2014, only around six percent of the 21,000 objects the size of a football or larger in Earth orbit were active satellites – the rest was some form of space debris.[8] As the number of objects in space continues to grow, the hazards of space operation will likewise increase. These hazards place an increased emphasis on the successful tracking of active satellites and space debris alike. As an integral aspect of successful tracking and orbit prediction, ballistic coefficient estimation has been a major topic of study in recent years. Because MR SAT's stereoscopic imager is designed to image uncooperative resident space objects (URSOs), successful estimation of the ballistic coefficient of MRS SAT applies directly to this problem.

As the majority of objects in space can only be located using ground-based tracking, many ballistic coefficient estimation methods employ Two-Line Element (TLE) sets. Methods, such as those developed by Saunders et. all and Sang et. all, use these sets to estimate ballistic coefficient by comparing the change in semimajor axis provided by TLE data to the change propagated using initial conditions derived from the TLE.[9,10] Other methods, such as the one developed by Gupta and Anilkumar, minimize the differences in apogee and perigee altitudes to develop a best-case prediction for ballistic coefficient.[11] It is worth noting that these methods all assume a constant ballistic coefficient, which does not account for area variation due to tumbling objects. It is possible to further increase the accuracy of an estimate by accounting for tumbling, although the accuracy gains diminish with lengthening propagations.[12]

As ballistic coefficient estimation for the MR and MRS SAT mission will be conducted entirely using downlinked relative position data, real-time estimates of ballistic coefficient are possible. In the approach suggested by Mahajan et. all for the MR and MRS SAT mission, MR SAT would estimate its own ballistic coefficient using an Extended Kalman Filter (EKF), then employ an Unscented Kalman Filter (UKF) and differential drag effects to estimate the ballistic coefficient of

MRS SAT.[13] However, such an approach toward ballistic coefficient estimation requires computing power beyond the capabilities of MR SAT. Therefore, the approach taken in the following sections is to estimate the ballistic coefficient of MRS SAT using downlinked relative position and velocity data from MR SAT.

Approach

The process of estimating ballistic coefficient of an object from stereoscopic imaging data differs greatly from a similar process using TLE data. While TLE data may be available only sparsely and at irregular intervals, it is accessible for the entire lifetime of the spacecraft. Stereoscopic imaging data, on the other hand, is available in very regular intervals, but only for a short period of time – only three hours of relative position and velocity data are available for the MR and MRS SAT mission, in fifteen second intervals. In practice, this means certain oscillatory perturbing effects, such as Earth's J_2 perturbations, have an impact on the spacecraft's change in semimajor axis. Meanwhile, other effects, such as solar radiation pressure, become less important.

Similar to the method developed by Saunders, the method compares the change in semimajor axis derived from observational data to the change propagated using a perturbation model. As such, it assumes data are available in regular, evenly-spaced intervals for a short period when a spacecraft is under observation. Observational data are derived using estimates from MR SAT's EKF for its own position and MRS SAT's relative position. From these data, MRS SAT's inertial position can be estimated. One advantage of this method is that it does not require any knowledge the MR SAT spacecraft's ballistic coefficient or physical properties – MRS SAT's ballistic coefficient can be measured independently.

As with the TLE sets used in a variety of ground-based estimation methods, the relative position and velocity measurements processed onboard MR SAT are inherently noisy – current estimates place relative position uncertainty as high as 2 meters RMS, and relative velocity uncertainty as high at 0.01 m RMS. From these measurements, the semimajor axis of the spacecraft can be calculated instantaneously using the orbital energy equation

$$a = -\frac{\mu}{2(\frac{v^2}{2} - \frac{\mu}{r})} \tag{7}$$

where a is the instantaneous semimajor axis, μ is the gravitational parameter of Earth, v is the magnitude of the spacecraft's velocity, and r is the magnitude of the spacecraft's position vector. It should be noted that the semimajor axis derived from orbital energy is more prone to noise than the Kozai mean motion-derived seimajor axis returned in TLEs. In order to improve the semimajor axis observational data used in the ballistic coefficient estimation, a fourth-order least squares estimate is used to interpolate semimajor axis at some time t_k. This least squares estimate is fitted to $2n + 1$ data points ranging from t_{k-n} to t_{k+n}.

Additionally, as noted most specifically by Gondelach et. all, but also mentioned by others, a better signal-to-noise ratio can be achieved by picking two observation points farther apart.[14] Therefore, the algorithm that is the focus of this study selects two observation points spaced more than one orbit apart, then applies a least squares filter to determine semimajor axis at each point. From these two observation points, the change in semimajor axis, Δa is calculated as

$$\Delta a_{obs} = a_{1,obs} - a_{2,obs} \tag{8}$$

To determine the numerical change in ballistic coefficient, one common approach is to estimate a' at several discrete points in the future, then numerically integrate to find the total Δa.[9] This method assumes that Δa_{obs} is solely attributable to atmospheric drag, which past studies have shown to be largely valid.[9] However, such an assumption also relies on the removal of long and short-term periodic effects achieved during the creation of a TLE. As these periodic effects have not been removed from MRS SAT's orbital data, the method outlined in this study estimates Δa from direct propagation between two points. The author is continuing to investigate optimum methods to limit noise in such a propagation. Using the direct propagation method, Δa_{prop} is given by

$$\Delta a_{prop} = a_{1,obs} - a_{2,prop} \tag{9}$$

Numerical estimation of ballistic coefficient from orbit propagation is an iterative process achieved using a combination of the bisection and secant methods. As the high levels of noise inherent in shorter propagations sometimes prevent a good first and second secant method guess, the bisection method is used to generate the first two guesses for ballistic coefficient. For each of these initial guesses a comparison parameter is generated, where

$$\delta a(\beta_j) = \Delta a_{prop} - \Delta a_{obs} \tag{10}$$

Once two initial guesses for ballistic coefficient and the associated comparison parameter have been generated, the secant method is employed until final convergence is reached, where convergence is marked by $\delta a(\beta_j) < 10^{-6}$. Ballistic coefficient is updated as

$$\beta_{j+1} = \beta j - 1 - \frac{\delta a(\beta_j)[\beta_j - \beta_{j-1}]}{\delta a(\beta_j) - \delta a(\beta_{j-1})} \tag{11}$$

Typically, the algorithm converges within four iterations. Once ballistic coefficient has been estimated for a single time interval, t_1 and t_2 are moved forward by one time step, and the ballistic coefficient is re-calculated. This process is repeated until ballistic coefficient has been calculated from all stereoscopic imaging data.

From this collection of discrete ballistic coefficient values, it is desirable to obtain a single ballistic coefficient estimation. However, the mean and median of this set can be highly susceptible to outliers. Therefore, the approach taken by Saunders et. al to estimate ballistic coefficient from a discrete set of values is mirrored here. In their approach, they attempt to eliminate noise in the calculation by taking the most common value of ballistic coefficient. This value is estimated by using a Gaussian function to generate a continuous histogram from a discrete set of ballistic coefficient values, then taking the maximum to be the location of the most common ballistic coefficient value.[9] This Gaussian function is given by

$$g(x,\beta) = \frac{1}{n} e^{-(\frac{x-\beta}{\beta_m})^2} \tag{12}$$

where n is the number of ballistic coefficient estimates generated, x is the variable along which the distribution is plotted, and β_m is the mean of the set of ballistic coefficient estimations.

In summary, the algorithm for estimating ballistic coefficient from stereoscopic imaging data follows as

while *Not all data processed* **do**
  Calculate Δa_{obs};
  while $\delta a(\beta_j) > 10^{-6}$ **do**
    if *Less than two guesses* **then**
      Find β_{j+1} using the bisection method;
    else
      Find β_{j+1} using the secant method;
    end
  end
end
Estimate β according to the most common value;

Algorithm 1: Estimating ballistic coefficient from relative position data

Results and Analysis

Table 2 shows the results of the algorithm found using the 1976 Standard Atmosphere-based drag model outlined in this paper. Position and velocity data were generated for 3 hours in 15-second intervals, then corrupted with a 2 m standard deviation in the x, y, and z directions for position, and 0.01 m/s standard deviation in the x, y, and z directions for velocity. The algorithm used to estimate ballistic coefficient for this work considered 20 elements in its least squares estimates of semimajor axis, and used two-hour propagations for ballistic coefficient estimation.

Table 2: Ballistic Coefficient Estimation Data

Truth	Estimated Value	Std. Deviation	Error(%)
0.0500	0.0510	0.0253	2.00
0.0250	0.0280	0.0275	12.0
0.0167	0.0187	0.0251	11.9

As the table shows, the algorithm performed well on a range of ballistic coefficient values. One interesting trend observed in the data is the increase in error with decreasing ballistic coefficient, which indicates that estimating ballistic coefficient becomes more difficult as the effect of drag on the spacecraft decreases. Anecdotal evidence also suggests that error could be reduced by further tuning the least squares estimate and propagation time. It should also be noted that simulated data are not a substitute for actual orbit data. Therefore, the next step in the algorithm's development will be to test it against on-orbit data from a variety of spacecraft, before it is applied to the MR and MRS SAT mission.

CONCLUSION

In this paper, a brief overview of the methodology related to spacecraft drag analysis was presented. From this knowledge, a drag model intended for mission design and planning, particularly in the university setting, was developed. The model was equipped with a variety of tools to enhance functionality and flexibility. Potential applications were also discussed.

The model was applied to a several challenges related to the MR and MRS SAT mission. First, it was used to perform a differential drag analysis on the MR and MRS SAT spacecraft, with special focus applied to collision avoidance. Qualitative evidence indicated that, even in the absence of end-of-life maneuvers, the MR and MRS SAT spacecraft are unlikely to collide due to the coupling of position and velocity inherent in a circumnavigation orbit. The model was also applied to the problem of ballistic coefficient determination using stereoscopic imaging data of MRS SAT. Methods developed for ground-based ballistic coefficient estimations using TLE data were adapted for space-based measurements. Tests of this algorithm using simulated data indicated promising results.

FUTURE WORK

In the future, the drag model detailed in this work will be released to the M-SAT team, with a potential public

release to follow. The author also intends to further develop the ballistic coefficient estimation algorithm using STK simulation and real-world spacecraft data.

ACKNOWLEDGEMENTS

The authors thank the AFRL University Nanosatellite Program, AFRL, and AFOSR for their continuing technical mentoring and financial support. Donna Jennings and the rest of Dr. Pernicka's Ph.D. students are also acknowledged for their advice and support.

REFERENCES

1. D. M. Prieto, B. P. Graziano, and P. C. E. Roberts, "Spacecraft Drag Modelling," *Progress in Aerospace Sciences*, vol. 64, pp. 56–65, 2014.
2. D. A. Vallado and D. Finkleman, "A Critical Assessment of Satellite Drag and Atmospheric Density Modeling," *Acta Astronautica*, vol. 95, pp. 141–165, 2014.
3. L. Sagnières and I. Sharf, "Uncertainty Characterization of Atmospheric Density Models for Orbit Prediction of Space Debris," *Proceedings of the 7th European Conference on Space Debris*, 2017.
4. K. Riesing, "Orbit Determination from Two Line Element Sets of ISS-Deployed CubeSats," *Proceedings of the 29th Annual AIAA/USU Conference on Small Satellites*, 2015.
5. C. Foster, H. Hallam, and J. Mason, "Orbit Determination and Differential-Drag Control of Planet Labs CubeSat Constellations," *AAS/AIAA Advances in Astronautical Sciences Series*, vol. 156, 2015.
6. B. Lewis, "Complete 1976 Standard Atmosphere," 2007.
7. "U.S. Standard Atmosphere," 1976.
8. L. Hall, "The History of Space Debris," *Space Traffic Management Conference*, 2014.
9. A. Saunders, G. G. Swinerd, and H. G. Lewis, "Deriving Accurate Satellite Ballistic Coefficients from Two-Line Element Data," *Journal of Spacecraft and Rockets*, vol. 49, pp. 175–184, 2012.
10. J. Sang, J. C. Bennett, and C. H. Smith, "Estimation of Ballistic Coefficients of Low Altitude Debris Objects from Historical Two Line Elements," *Advances in Space Research*, vol. 52, pp. 117–124, 2013.
11. S. Gupta and A. K. Anilkumar, "Integrated Model for Prediction of Reentry Time of Risk Objects," *Advances in Space Research*, vol. 52, pp. 295–299, 2015.
12. R. Russell, N. Arora, V. Vittaldev, D. Gaylor, and J. Anderson, "Ballistic Coefficient Prediction for Resident Space Objects," *Proceedings of the Advanced Maui Optical and Space Surveillance Technologies Conference*, vol. 1, 2012.
13. B. Mahajan, H. J. Pernicka, and J. Darling, "Orbit Determination of an Uncooperative RSO Using a Stereo Vision-Based Sensor," *Proceedings of the 23rd AAS/AIAA Space Flight Mechanics Meeting*, 2013.
14. D. J. Gondelach, R. Armellin, and A. A. Lidtke, "Ballistic Coefficient Estimation for Reentry Prediction of Rocket Bodies in Eccentric Orbits Based on TLE Data," *Mathematical Problems in Engineering*, vol. 2017, 2017.